Relationship between element-selective electronic states and hydrogen absorption properties of Pd-M (M = Ru, Rh, Ag, and Au) alloys

Kanako Fujii,[1] Naoki Ishimatsu,[1,*] Hiroshi Maruyama,[1] Tatsuya Shishidou,[2,†] Shinjiro Hayakawa,[3] and Naomi Kawamura[4]

[1]*Department of Physics, Graduate School of Science, Hiroshima University, 1-3-1 Kagamiyama, Higashihiroshima, Hiroshima 739-8526, Japan*

[2]*Graduate School of Advanced Sciences of Matter (ADSM), Hiroshima University, 1-3-1 Kagamiyama, Higashihiroshima, Hiroshima 739-8530, Japan*

[3]*Department of Applied Chemistry, Graduate School of Engineering, Hiroshima University, Higashihiroshima, Hiroshima 739-8527, Japan*

[4]*Japan Synchrotron Radiation Research Institute (JASRI), SPring-8, 1-1-1 Kouto, Sayo-cho, Sayo-gun, Hyogo 679-5198, Japan*

(Received 4 August 2016; revised manuscript received 8 November 2016; published 30 January 2017)

To understand how the constituent atoms participate in the hydrogenation of Pd-based alloys at ∼0.1 MPa of hydrogen pressure (P_{H_2}), we investigated the electronic states in Pd-M (M = Ru, Rh, Ag, and Au) alloys and their hydrides element-selectively by using x-ray absorption spectroscopy at the $L_{2,3}$ edges. Spectral changes near the absorption edge demonstrate that both Pd and M atoms form bonds with H atoms in the Pd-M (M = Ru and Rh) alloys even at $P_{H_2} \sim 0.1$ MPa. This is a striking result because high pressures of more than 1 GPa are required for the hydrogenation of Rh and Ru pure metals. In contrast, only Pd atoms bond with H atoms and the M-H bond is absent in the case of Pd-M (M = Ag and Au) alloys. Therefore, the hydrogen-induced changes in the electronic states differ between Ms with fully occupied d shells and Ms with partially occupied d shells. This study reveals that the thermodynamic hydrogenation properties of Pd-M alloys can be determined by a combination of the formation of the M-H bond and lattice expansion or compression by alloying Pd metal with M.

DOI: 10.1103/PhysRevB.95.024116

I. INTRODUCTION

Palladium (Pd) is an important material for the hydrogen absorbing alloys [1,2]. Molecular H_2 dissociates at the surface of Pd, the atomic H occupies octahedral sites in the fcc lattice of Pd metal, and Pd monohydride (PdH), which has a NaCl-type structure, is formed. At room temperature, the β phase of PdH_x ($x \sim 0.6$) coexists with the α phase of PdH_x ($x \leqslant 0.1$), which is present as a solid solution, at an equilibrium hydrogen pressure of $P_{H_2} \leqslant 1$ kPa. The coexistence is observed as a plateau of P_{H_2} in the P-x curve. The high activity of Pd with hydrogen is of great interest, because other d metals with more than half-filled d shells such as Ru and Rh are hydrogenated at P_{H_2} values exceeding 1 GPa to form the β phase [3,4]. The difference in molar enthalpy at the hydrogenation, ΔH_{plat}, of Pd is estimated to be -40 kJ/mol H_2 [1]; the negative value ΔH_{plat} is indicative of the high stability of the β phase of PdH_x compared with that of the α phase.

The excellent hydrogen absorbing properties of Pd metal are modified by alloying Pd with another transition metal M. In the case of M = Rh, P_{H_2} increases rapidly with increasing Rh content, and the hydrogen content x of the β phase of the Pd-Rh alloy slightly increases [5]. This trend of P_{H_2} indicates that ΔH_{plat} also increases and the sign of ΔH_{plat} eventually becomes positive [see Fig. 9(b)]. Consequently, the $Pd_{1-y}Rh_y$ alloy with Rh content $y \geqslant 0.1$ is no longer hydrogenated at pressures lower than $P_{H_2} \sim 0.1$ MPa. In the case of M = Ag, P_{H_2} decreases with increasing Ag content [6]. This result is due to a decrease in ΔH_{plat}, so that the hydrogenation of the Pd-Ag alloy is more reactive than that of Pd metal; however, the β phase of the Pd-Ag alloy absorbs a lesser amount of hydrogen atoms than pure Pd. The plateau corresponding to the coexistence of α and β phases at P_{H_2} vanishes in the P-x curve at an Ag content greater than $y = 0.24$ of the $Pd_{1-y}Ag_y$ alloy; pressures much higher than $P_{H_2} \sim 0.1$ MPa are required to achieve hydrogenation of the Pd-Ag alloy to absorb the same amount of hydrogen in the β phase of pure Pd at 300 K.

Alloying Pd with the neighboring Rh or Ag metals in the fifth row of the periodic table, the average number of 4d electrons decreases or increases, respectively, in the alloy with respect to the number of pure Pd. Therefore, interpretations based on the rigid-band model have been widely used to understand the hydrogenation property of transition-metal alloys [7–10]. However, the nonsystematic behavior of the hydrogenation as a function of Rh and Ag content demonstrates that the rigid-band model is an oversimplified interpretation of the hydrogenation properties; the intrinsic H absorbing property of each M atom probably influences the hydrogenation of the Pd-M alloys. However, it is not fully understood how Rh and Ag atoms participate in the hydrogenation of the Pd-M alloys.

In this paper, we have investigated the d electronic states of Pd-M alloys (M = Ru, Rh, Ag, and Au) before and after hydrogenation by using x-ray absorption spectroscopy (XAS) at the L_2 and L_3 edges. The XAS profile at the $L_{2,3}$ edges is capable of detecting the reconstruction of the d and s unoccupied electronic structures above the Fermi energy (E_F) due to hydrogenation [11–13]. XAS has the advantage that the partial electronic structures of Pd and M can be distinguished by tuning the photon energies to the absorption edges of these elements. Therefore, XAS analysis allows us to discuss the element-selective influence of the constituent atoms on the hydrogenation of the Pd-M alloys. We have also

*ishimatsunaoki@hiroshima-u.ac.jp

†Present address: Department of Physics, University of Wisconsin–Milwaukee, Milwaukee, Wisconsin 53201, USA.

performed first-principles calculations to elucidate the spectral changes due to hydrogenation. Finally, the hydrogenation properties of the Pd-M alloys are discussed based on the relationship between the element-selective electronic structure and thermodynamic properties.

II. EXPERIMENTAL PROCEDURE

Pd-M (M = Ru, Rh, Ag, and Au) polycrystalline alloys were synthesized by the arc melting method. The obtained ingots were cut and formed into disks 0.3 mm in thickness. The actual composition of each alloy was evaluated by electron-probe microanalysis. The disk was hydrogenated under a flow of H_2 gas at 0.1 MPa and room temperature. X-ray diffraction was measured *in situ* to monitor volume expansion during the hydrogenation process. The lattice constant linearly increased from 3.8907 to 4.090 Å on the hydrogenation from Pd metal to PdH monohydrides [14]. This trend allows us to suppose the relationship between the hydrogen content x and the volume expansion: $x = (a_{MH} - a_M)/0.20$, where a_M and a_{MH} are the lattice constants before and after hydrogenation, respectively, in units of Å. Applying the same relationship to the Pd-M alloys, we evaluated the hydrogen content of each alloy. Lattice constants of the fcc structure consisting of disordered Pd and M atoms were used as the input values for this estimation.

XAS measurements at the $L_{2,3}$ edges of the 4d elements were performed on BL-11 of Hiroshima Synchrotron Research Center (HSRC) [15]. XAS spectra at the Au $L_{2,3}$ edges were measured on BL39XU of SPring-8 [16]. Spectra at the Pd $L_{2,3}$ edge were recorded using the conversion electron yield (CEY) method, whereas partial fluorescence yield (PFY) was employed to measure spectra at the $L_{2,3}$ edges of other Ms by using a silicon drift detector. Samples were exposed to a flow of 95%He+5%H_2 gas during the XAS measurements on BL-11 to avoid hydrogen desorption. On the other hand, samples were enclosed in an H_2 atmosphere at 0.1 MPa during the XAS measurements on BL39XU for the same purpose. Using XRD measurements, we confirmed that significant hydrogen desorption did not occur; that is, more than 90% of the initial hydrogen content remained in the sample after the XAS measurements. It should be noted that CEY is a surface-sensitive technique, which has a probing depth on the order of several tens of nm, and this depth is significantly thinner than the probing depth of PFY, which is typically on the order of μm. Hydrogen-induced changes were observed in both spectra obtained by CEY and PFY. This observation ensures that hydrogen atoms occupy the whole part of the sample, and that severe segregation does not occur.

The density of states (DOS) of the M hydrides and XAS profiles were calculated using first-principles calculations based on density functional theory with the all-electron full-potential linear augmented plane-wave method [17]. Exchange and correlation were treated with the generalized gradient approximation. Uniform k-mesh sets of $40 \times 40 \times 40$ with the improved tetrahedron method were used for integration in the Brillouin zone. Spin-orbit interaction is included self-consistently. The muffin-tin sphere radii were set to 1.1 Å for M and 0.85 Å for H. The transition probability per unit time based on Fermi's golden rule was calculated in order to simulate the XAS spectra. The transition matrix elements were calculated only taking into account the electric dipole transitions. The effect of core hole potential was ignored in these calculations.

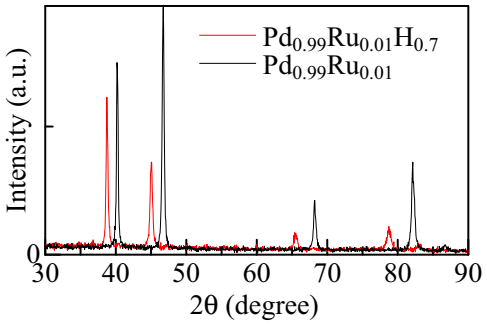

FIG. 1. XRD patterns of the polycrystalline $Pd_{0.99}Ru_{0.01}$ disk (black) and its hydride (red). A Cu $K\alpha$ x ray was used for the measurements.

III. RESULTS AND DISCUSSION

A. Hydrogen absorbing property of the Pd-M alloys

XRD patterns of a polycrystalline $Pd_{0.99}Ru_{0.01}$ disk and its hydride are shown in Fig. 1 as an example of hydrogenation. Both diffraction patterns are assigned as fcc structures because x-ray scattering from hydrogen atoms is very weak. The pattern of the hydride shifts to lower angles due to volume expansion of hydrogenation. The width of the Bragg peak becomes ~1.2 times broader after hydrogenation, which is induced by the local strain of Pd/Ru atoms around hydrogen atoms. The composition dependence of the lattice constant of the Pd-M alloys is summarized in Fig. 2. The hydrogenation-induced volume expansion is also displayed in this figure. The lattice constant changes linearly by alloying Pd with Ms. Alloying with Au, Ag, and Pt metals expands the lattice constant, whereas other Ms (Cu, Rh, and Ru) decrease the lattice constant. This systematic trend is attributed to Vegard's law based on the relative difference of the atomic radius of M with respect to Pd.

The large volume expansion due to hydrogenation is clearly shown in Fig. 2. As mentioned in the previous section, we evaluated the hydrogen content of each alloy under the conditions of $P_{H_2} \sim 0.1$ MPa and 300 K based on the hydrogen-induced volume expansion: $x = (a_{MH} - a_M)/0.20$. The inset of Fig. 2 summarizes the hydrogen content, x, as a function of M content, y. The average error for x, which is calculated from the full width at half maximum of Bragg peaks, is estimated to be ~2%. The value of x moderately decreases with increasing y for Cu, Ag, and Au contents. In the case of the Pd-Rh alloy, a sudden drop in x occurs when y reaches ~0.15; this drop appears after a slight increase in x with increasing Rh content up to $y = 0.12$. A steep decrease in x is observed in the case of the Pd-Ru and Pd-Pt alloys. The steep decrease and sudden drop in x correspond to the fact that P_{H_2} increases with increasing M content and exceeds 0.1 MPa. The slight increase in x compared with that of pure Pd has been reported not only for the Pd-Rh alloy but also for the Pd-Ru alloy; hydrogen content up to $x = 0.8$ has been observed in the $Pd_{0.98}Ru_{0.02}$ alloy by the magnetic susceptibility [7] and

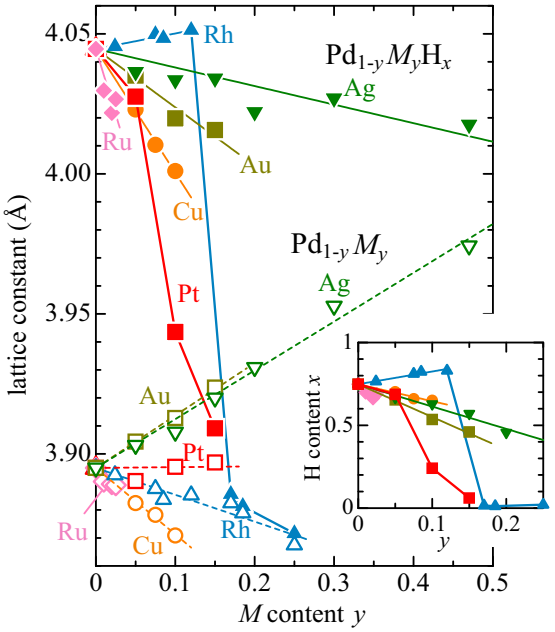

FIG. 2. Lattice constant of Pd-M alloys as a function of M content y. Open symbols represent the lattice constants before hydrogenation, and closed symbols denote the lattice constants after hydrogenation. Solid and broken lines are guides for the eye. The inset shows hydrogen content x as a function of y. The hydrogen content, x, was evaluated from the hydrogen-induced expansion of lattice constants.

voltammogram [18] measurements. However, a Pd-Ru alloy with additional hydrogen content was not obtained in our sample preparation.

B. DOS and calculated XAS spectra

Figure 3 shows the DOS of Ag, Pd, Rh, and Ru monohydrides together with those of the pure metals. To examine the influence of hydrogen occupancy on the element-selective electronic structure in the Pd-M alloys, we calculated the DOS of Ru, Rh, Ag, and their monohydrides by assuming fcc and NaCl-type crystal structures, respectively. The same lattice constants for PdH (4.090 Å) and the fcc structure of the Pd lattice (3.8907 Å) were used for our calculations of MH and M, respectively. Our calculations of Pd and PdH well reproduce the results of the earlier theoretical work [19]. The large DOS near the E_F mainly consists of a 4d component originating from the overlap of M 4d orbitals of neighboring sites. We refer to this as the 4d band hereafter.

Changes in the DOS due to hydrogenation are summarized as follows.

(i) Bonding and antibonding states appear below and above the 4d band. These states consist of hybridization between M s,p,4d, and H 1s components. The bonding and antibonding states of RuH, RhH, and PdH are located at $\sim E_F - 7$ and $\sim E_F + 5$ eV, respectively. Concerning AgH, the bonding and antibonding states appear at lower-energy levels.

(ii) The 4d band narrows. This is caused by reduced overlap between M 4d orbitals due to the hydrogenation-induced volume expansion.

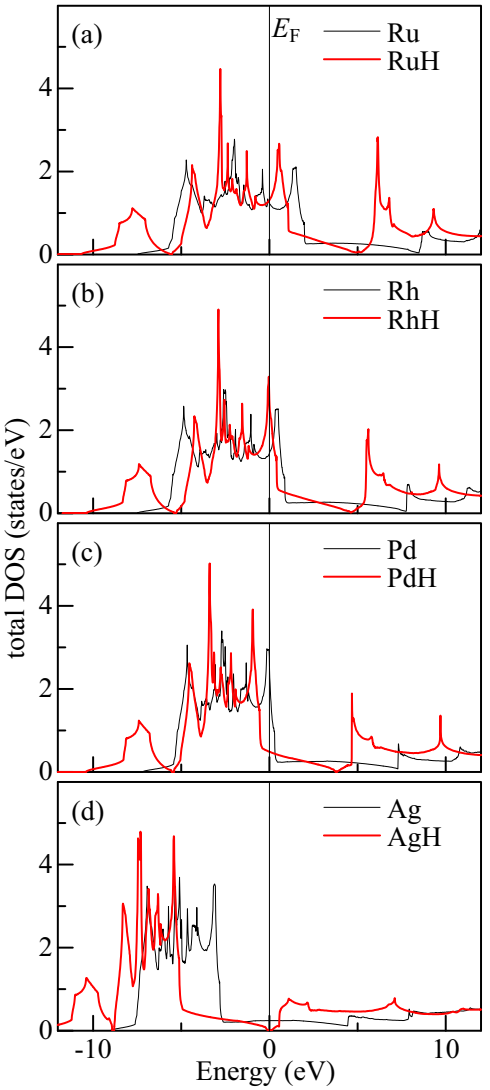

FIG. 3. Total DOS of (a) AgH, (b) PdH, (c) RhH, and (d) RuH (red, thick lines) together with the DOS of pure metals (black, thin lines). The vertical lines indicate the Fermi energy, E_F.

(iii) The Fermi energy, E_F, changes with respect to the 4d band. E_F moves to the higher-energy part of the 4d band, and the E_F of PdH is located above the 4d band [19].

Concerning the reconstruction of the electronic state after hydrogenation, it is well known that the electron density around the H atom in a metal hydride becomes noticeably higher than that around an isolated H atom. The attractive electrostatic potential of the proton causes the bonding state accommodating two electrons, where the charge density is spherically distributed (s character) around the proton [20,21]. However, the total number of 4d electrons is almost unchanged after hydrogenation, which is in contrast to the drastic changes in the location of E_F with respect to the 4d band. The increase in the number of 4d electrons in the muffin-tin spheres is estimated to be $\sim$0.1 or less. The extra electrons around the proton originate from the interstitial charge density of the M s and p conduction electrons that are mainly distributed outside of the muffin-tin spheres. Therefore, the number of electrons in the muffin-tin spheres does not change significantly.

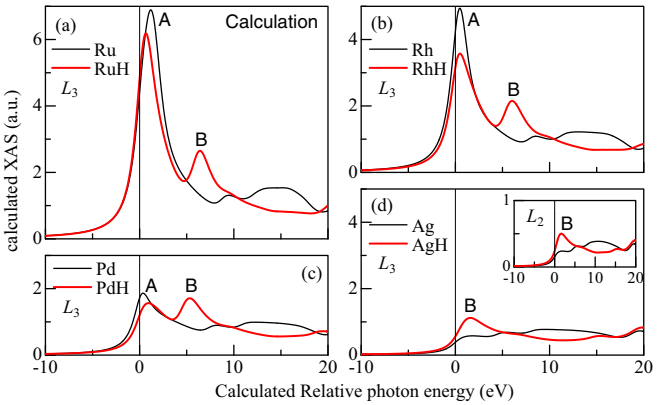

FIG. 4. Calculated XAS profiles of (a) RuH, (b) RhH, (c) PdH, and (d) AgH at the M L_3 edge (red, thick lines) together with XAS of pure metals (black, thin lines). The vertical lines indicate the absorption edge E_0 determined from the energy gap between the $2p_{3/2}$ core level and Fermi energy of the M. The inset in panel (d) displays calculated profiles of Ag and AgH at the Ag L_2 edge.

In Fig. 4, the calculated XAS profiles of pure metals and monohydrides at the M L_3 edge and Ag L_2 edge are plotted for comparison with the results of experiments. Photon energies of Fig. 4 are simply plotted as relative energies with respect to the energy gap between the $2p_{3/2}$ core level and the Fermi energy of the pure metal (M). The following three modifications are recognized in the XAS profile as resulting from the H-induced reconstruction of the electronic structure: (i) suppression of the white line (WL), labeled as A; (ii) the appearance of a new peak, labeled as B; and (iii) the shift of the absorption edge. Because the integrated intensity of the WL corresponds to the number of 4d holes [22], the suppression of WL indicates that the number of unoccupied states in the 4d band near the E_F decreases after hydrogenation. The new peak B, which appears about 7 eV above the absorption edge, is attributed to the antibonding states consisting of the M 4d and H 1s orbitals. The shift of the absorption edge due to the hydrogenation is estimated to be +0.4 eV at the Pd L_3 edge, whereas the shift is small in the cases of Rh and gives a negative value for Ru. The spectral change of Ag significantly differs from those of Ru, Rh, and Pd. WL does not exist in the profile of Ag because the 4d band is fully occupied. However, our calculations predict that a prominent peak should appear near the absorption edge after hydrogenation if AgH is formed. According to the DOS of AgH, this new peak should be assigned to peak B, corresponding to the antibonding state, because the antibonding state appears near the E_F.

C. XAS profile at the $L_{2,3}$ edges of the 4d and 5d elements

Experimental results of XAS spectra are shown in Figs. 5–8. Figure 5 shows hydrogenation-induced changes in the XAS spectra of pure Pd and Pd-M alloys at the Pd $L_{2,3}$ edges. Three changes predicted by the calculation were observed in the experimental XAS profiles as a result of the H-induced reconstruction of the local electronic states around Pd: (i) suppression of WL, labeled as A; (ii) the appearance of a new peak, labeled as B; and (iii) the shift of the absorption edge to higher energy, as plotted in the inset of Fig. 5. These three

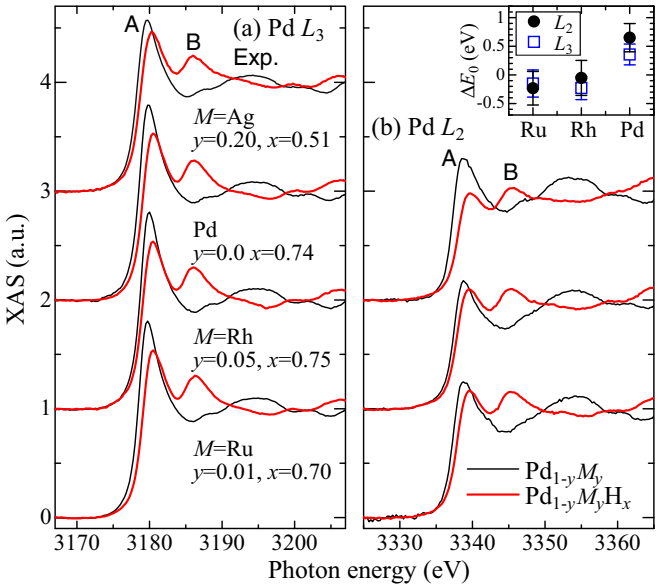

FIG. 5. XAS spectra of Pd, Pd-M alloys and their hydrides at the Pd $L_{2,3}$ edges. Thin (black) lines and thick (red) lines represent the spectra of alloy and hydrides, respectively. The inset in the right panel summarizes the energy shift of the absorption edge E_0 at M $L_{2,3}$ edges after hydrogenation.

changes are observed at the Pd L_2 and L_3 edges of all samples, indicating that Pd atoms bond with the H atoms in each alloy. The bond corresponds to hybridization of electronic orbitals between M d, p, s, and H 1s electrons due to bonding and antibonding states.

Figures 6 and 7 show XAS spectra of Pd-Rh alloys at the Rh $L_{2,3}$ edges and the spectra of Pd-Ru alloys at the Ru $L_{2,3}$ edges, respectively. The intensity of the WL is larger than that of the Pd $L_{2,3}$ edges because of the reduced number of 4d electrons in Rh and Ru atoms. The suppression of WL and

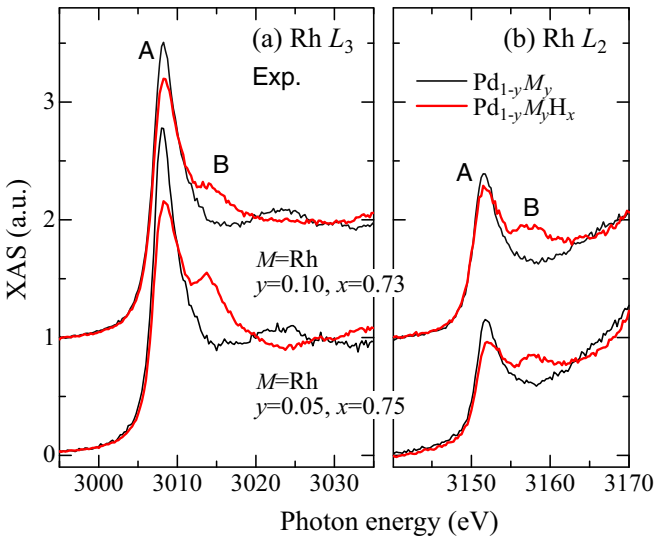

FIG. 6. XAS spectra of the Pd-Rh alloys at the Rh $L_{2,3}$ edges. Thin (black) lines and thick (black) lines represent the spectra of alloys and hydrides, respectively.

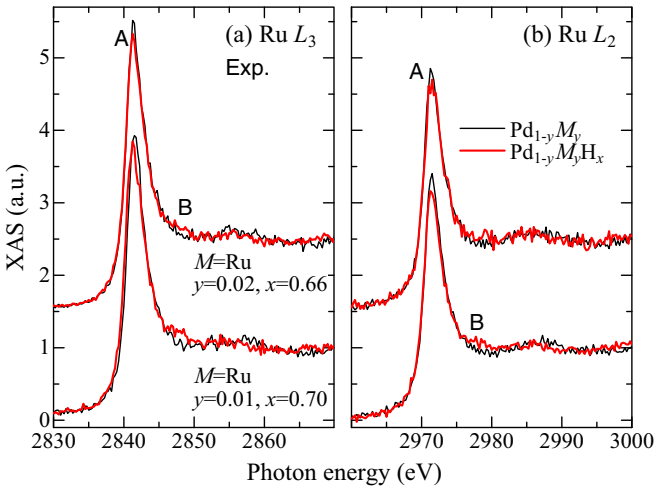

FIG. 7. XAS spectra of the Pd-Ru alloys at the Ru $L_{2,3}$ edges. Thin (black) lines and thick (red) lines represent the spectra of alloy and hydrides, respectively.

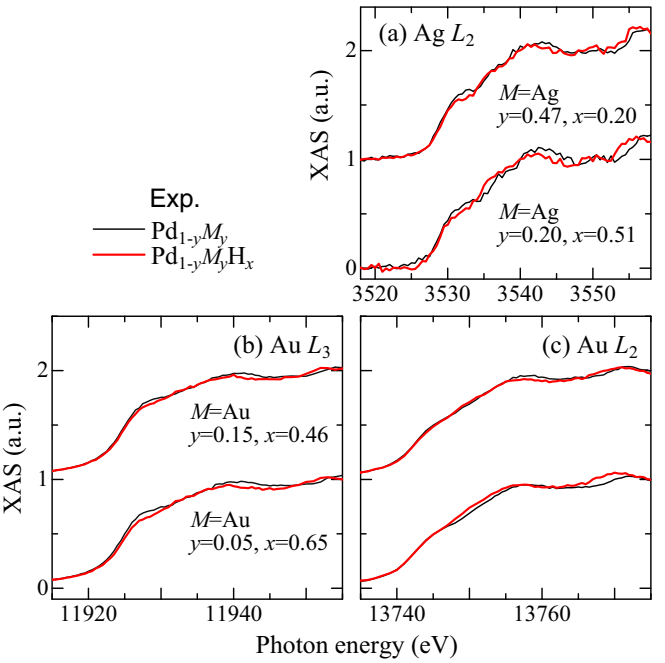

FIG. 8. XAS spectra of the Pd-M (M = Ag, Au) alloys at the (a) Ag L_2, (b) Au L_3, and (c) Au L_2 edges. Thin (black) lines and thick (red) lines represent the spectra of alloy and hydrides, respectively.

the newly formed peak B are as hydrogen-induced changes, and these are similar to the spectral changes at the Pd $L_{2,3}$ edges. As summarized in the inset of Fig. 5, the absorption edge moves towards lower energy or is unchanged at the Rh and Ru $L_{2,3}$ edges after hydrogenation, which is in contrast to the remarkable positive shift at the Pd $L_{2,3}$ edges.

These spectral changes reveal that, by alloying Pd with Ru or Rh, Rh-H and Ru-H bonds are formed even under $P_{H_2} \sim 0.1$ MPa. The appearance of Ru-H and Rh-H bonds in the Pd-M alloys is a striking result of this study because high pressures of more than 1 GPa are required for the hydrogenation of Rh and Ru pure metals. The excellent reproducibility of the experimental XAS profiles at the Rh L_3 edge by the calculated spectra based on the Rh monohydrides demonstrates that the partial electronic states of Rh in the alloy are mostly similar to the electronic state of their monohydrides. In the $Pd_{0.95}Rh_{0.05}H_{0.7}$ alloy, the Rh atoms bond with four or five neighboring H atoms at octahedrally coordinated sites, which yields a nearly same electronic structure due to the coordination around the Rh atoms in Rh monohydride with the NaCl structure. On the other hand, we note that the experimental profiles at the Ru $L_{2,3}$ edges exhibit a small decrease in the WL intensity and a low-intensity B peak; compared with the calculated profile at the Ru L_3 edge (see Fig. 4), the changes in the experimental profile are suppressed. The weak changes indicate that the Ru atoms in the Pd-Ru alloy are surrounded by fewer H atoms than the number of H atoms around Pd and Rh atoms, and Ru atoms probably form weak bonds with H atoms. We speculate that H atoms preferentially occupy Pd-rich sites in the Pd-Ru alloy, because the Ru-H bond is less stable than the Pd-H and Rh-H bonds.

As shown in Fig. 8, hydrogenation-induced changes in the XAS spectra at the Ag L_2 edge differ from those in the XAS profiles at the $L_{2,3}$ edges of other 4d elements. The oscillating profile above the edge moves to the lower-energy direction, which is due to the volume expansion after hydrogenation. The experimental profile after hydrogenation does not exhibit a peak in contrast to the fact that our calculations predict the appearance of peak B near the absorption edge. The small spectral change and the absence of peak B are also observed in the results at the Au L_2 and L_3 edges. Therefore, the electronic states of Ag and Au atoms are not influenced by hydrogen occupation. In the case of elements with fully occupied d shells such as Ag and Au, H atoms do not bond with Ag or Au atoms, and only Pd atoms bond with H atoms in the alloys at $P_{H_2} \sim 0.1$ MPa.

As shown in Fig. 5 and in the inset of the same figure, the absorption edge at the Pd $L_{2,3}$ edges shifts to higher energy, and this behavior is not observed at the $L_{2,3}$ edges of Rh and Ru. To understand the remarkable shift in the absorption edges, we paid attention to how the changes in the DOS affect the profiles near the edge. This is a valid approach because the experimental observation of the shift is well reproduced by the calculated spectra of Pd, as shown in Fig. 4. According to the DOS of Rh and Ru and their monohydrides, E_F is located within the 4d band, and high densities near the top of the 4d band remain unoccupied before and after hydrogenation. The presence of high unoccupied densities near the top of the 4d band results in the steep rising edge of the WL. In the case of Pd, the E_F of Pd moves above the 4d band after hydrogenation, and consequently the 4d band of PdH is fully occupied. The fully occupied 4d band of PdH yields a different absorption profile near the rising edge. Only low and uniform densities remain above the E_F of PdH, giving rise to the moderate slope of the rising edge near the absorption edge [12]. The difference between the moderate and steep slope at the rising edge results in the remarkable positive shift of the absorption edge. Therefore, the position of the absorption edge is determined from the H-induced change in the 4d band.

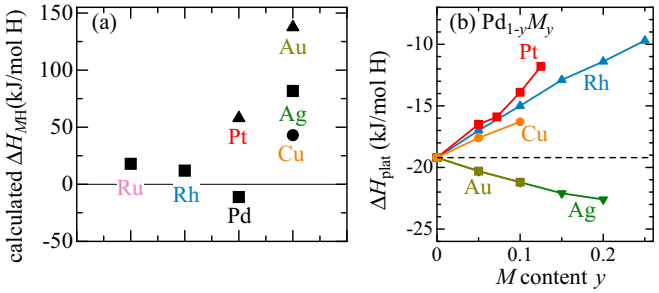

FIG. 9. (a) Calculated enthalpies, ΔH_{MH}, of Ms for the reaction $M + \frac{1}{2}H_2 + \Delta H_{MH} = MH$. (b) The M composition dependence of the relative enthalpies ΔH_{plat} for Pd-M alloys experimentally determined elsewhere. These enthalpies are evaluated from the plateau pressures P_{H2} of each alloy. The ΔH_{plat} of pure Pd is indicated by the horizontal dashed line. Each value of ΔH_{plat} is taken from Ref. [23] for Cu and Au, Ref. [24] for Pt, Ref. [6] for Ag, and Ref. [25] for Rh.

D. Relationship between hydrogenation properties and the element-specific electronic structure

In this subsection, we discuss the relationship between the thermodynamic hydrogenation properties and the element-specific electronic structure of the Pd-M alloy. Our first-principles calculations evaluate the energy difference, ΔQ, between M and MH. By subtracting the Gibbs free energy of hydrogen gas, -15.87 eV/H atom at 300 K from ΔQ, the enthalpy of formation, ΔH_{MH}, is estimated as a thermodynamic parameter from the following reaction; $M + \frac{1}{2}H_2 + \Delta H_{MH} = MH$. The evaluated values of ΔH_{MH} are plotted in Fig. 9(a). Only the reaction of Pd with hydrogen gives a negative value of ΔH_{MH}; other M metals yield positive values of ΔH_{MH}. The negative ΔH_{MH} of Pd is demonstrated by the exothermic nature of the hydrogenation reaction.

The calculated values of ΔH_{MH} demonstrate that the formation of M-H bonds (M = Ru, Rh, and Ag) is endothermic, and the M-H bonds are energetically unstable compared with the stability of Pd-H bonds. Our results of XAS reveal that both Rh-H and Ru-H bonds exist together with the Pd-H bonds in the Pd-Rh and Pd-Ru alloys, even at $P_{H_2} \sim 0.1$ MPa, so that endothermic reactions due to the formation of Rh-H or Ru-H bonds compensate for the exothermic reaction for the formation of the Pd-H bonds in the Pd-M alloy. Therefore, an increase in the number of Rh-H or Ru-H bonds increases the enthalpy of the reaction, ΔH_{plat}. Consequently, the hydrogenation of Pd-Rh and Pd-Ru alloys eventually becomes endothermic, as illustrated in Fig. 9(b).

On the other hand, the values of ΔH_{plat} for the Pd-Ag and Pd-Au alloys decrease with increasing Ag or Au content, which is the opposite trend of the hydrogenation of the Pd-Rh alloy. The XAS spectra at the Ag and Au $L_{2,3}$ edges reveal that Ag and Au atoms do not form bonds with H atoms in the alloy; only Pd atoms form bonds to H atoms. Because the number of Pd-H bonds decreases with increasing Ag or Au content, the H content, x, linearly decreases as shown in the inset of Fig. 2. To understand the origin of the enhanced negative ΔH_{plat}, it is valuable to note that ΔH_{plat} of the Pd-Cu alloy increases with increasing Cu content, which is the opposite trend to those of the Pd-Ag or Pd-Au alloys [23]. The different behavior between Cu, Ag, and Au alloys is surprising because Cu also has a closed 3d shell and Cu-H bonds are probably not present in the Pd-Cu alloy by analogy with the behavior in the Pd-Ag and Pd-Au alloys. One of the hints for understanding this opposite behavior is the lattice expansion (compression) that occurs on alloying Pd with elements with a larger (smaller) atomic radius. As shown in Fig. 2, the lattice parameter of the Pd-M alloy linearly increases with increasing Ag and Au contents, whereas the lattice parameter linearly decreases with increasing Cu contents because Cu has smaller atomic radius than Pd. Therefore, we concluded that the initial lattice expansion of the Pd-Ag and Pd-Au alloys has an influence on the enhanced negative ΔH_{plat}. Because occupation of hydrogen atoms typically causes a $\sim$5% expansion of lattice constant of the alloys, a significant amount of elastic energy is exhausted during hydrogenation. Therefore, the initial lattice expansion due to alloying with Ag and Au probably yields an energetic gain for the formation of Pd-H bonds in the alloy with respect to the energy required for a Pd-H bond in pure Pd. The changes in the enthalpy can also be understood by considering the changes in the effective electron density of the alloy, because importance of the low electron density for the hydrogenation has been proposed by the effective medium theory [26]. Ag and Au atoms do not bond with hydrogen; however, occupation of these atoms can be seen as *expanding* the Pd lattice and thereby decreasing the Pd electron density per volume unit. The lower electron density compared with that of Pd probably gives energetic gain to the hydrogenation of Pd-Au and Pd-Ag Alloys. Finally, we note that our interpretation is similar to the previous work of Fujitani *et al.* [27]. They have discussed the relationship between the equilibrium hydrogen pressure and lattice parameters for the $ZrMn_{2-x}M_x$ (M = V, Fe, Co, and Ni) system.

IV. CONCLUSIONS

In this paper, we have investigated the d electronic states of Pd-M alloys (M = Ru, Rh, Ag, and Au) before and after hydrogenation by using XAS at the $L_{2,3}$ edges. The relationship between the thermodynamic hydrogenation property of the Pd-M alloy and the element-selective electronic structure has been discussed. Spectral changes near the absorption edge demonstrate that both Pd and M atoms form bonds with H atoms in the Pd-M (M = Ru and Rh) alloys, whereas only Pd atoms form bonds with H atoms in the Pd-M (M = Ag and Au) alloys. Therefore, the effect of hydrogen on each M differs between the fully occupied and partially occupied d shells of the M. The existence of Ru-H and Rh-H bonds in the Pd-Ru and Pd-Rh alloys is a striking result of this paper, because Ru and Rh pure metals cannot be hydrogenated under $P_{H_2} \sim 0.1$ MPa. To summarize, the thermodynamic hydrogenation property ΔH_{plat} of the Pd-M alloys is determined by two phenomena as follows: (i) an increase in the number of M-H bond changes the negative value of ΔH_{plat} to positive values, and (ii) lattice expansion (compression) due to alloying Pd with M reduces (elevates) the values of ΔH_{plat}.

ACKNOWLEDGMENTS

The authors would like to thank Y. Matsushima, K. Kumamoto, and K. Mine for helpful discussions. We also thank Y. Shibata for the electron-probe microanalysis performed

at N-BARD, Hiroshima University. This work was partially supported by Grant-in-Aid for Scientific Research from JSPS, Japan (KAKENHI, Grant No. 25420756). Experiments at HiSOR were carried out under the approval of the Proposal Assessing Committee of the Hiroshima Synchrotron Radiation Center (Proposal Nos. 14-B-13 and 15-B-6). The XAS measurements at SPring-8 were performed with the approval of PRC-JASRI (No. 2014B1849).

[1] Y. Fukai, *The Metal-Hydrogen System*, 2nd ed. (Springer, Berlin, 2005).
[2] V. Antonov, J. Alloys Compd. **330–332**, 110 (2002).
[3] T. Scheler, M. Marqués, Z. Konôpková, C. L. Guillaume, R. T. Howie, and E. Gregoryanz, Phys. Rev. Lett. **111**, 215503 (2013).
[4] M. A. Kuzovnikov and M. Tkacz, Phys. Rev. B **93**, 064103 (2016).
[5] S. Thiebaut, A. Bigot, J. Achard, B. Limacher, D. Leroy, and A. Percheron-Guegan, J. Alloys Compd. **231**, 440 (1995).
[6] T. B. Flanagan, D. Wang, and S. Luo, J. Phys. Chem. B **111**, 10723 (2007).
[7] E. Wicke, J. Less-Common Metals **74**, 185 (1980).
[8] K. Kusada, M. Yamauchi, H. Kobayashi, H. Kitagawa, and Y. Kubota, J. Am. Chem. Soc. **132**, 15896 (2010).
[9] A. Yang, O. Sakata, K. Kusada, T. Yayama, H. Yoshikawa, T. Ishimoto, M. Koyama, H. Kobayashi, and H. Kitagawa, Appl. Phys. Lett. **105**, 153109 (2014).
[10] V. Antonov, M. Baier, B. Dorner, V. Fedotov, G. Grosse, A. Kolesnikov, E. Ponyatovsky, G. Schneider, and F. Wagner, J. Phys.: Condens. Matter **14**, 6427 (2002).
[11] M. W. Ruckman, G. Reisfeld, N. M. Jisrawi, M. Weinert, M. Strongin, H. Wiesmann, M. Croft, A. Sahiner, D. Sills, and P. Ansari, Phys. Rev. B **57**, 3881 (1998).
[12] I. Davoli, A. Marcelli, G. Fortunato, A. D'amico, C. Coluzza, and A. Bianconi, Solid State Commun. **71**, 383 (1989).
[13] N. Ishimatsu, R. Sasada, H. Maruyama, T. Ichikawa, H. Miyaoka, T. Kimura, M. Tsubota, Y. Kojima, T. Tsumuraya, T. Oguchi *et al.*, J. Phys.: Conf. Ser. **190**, 012070 (2009).
[14] Y. Wang, S. N. Sun, and M. Y. Chou, Phys. Rev. B **53**, 1 (1996).
[15] S. Hayakawa, Y. Hajima, S. Qiao, H. Namatame, and T. Hirokawa, Anal. Sci. **24**, 835 (2008).
[16] H. Maruyama, M. Suzuki, N. Kawamura, M. Ito, E. Arakawa, J. Kokubun, K. Hirano, K. Horie, S. Uemura, K. Hagiwara *et al.*, J. Synchrotron Rad. **6**, 1133 (1999).
[17] T. Tsumuraya, Y. Matsuura, T. Shishidou, and T. Oguchi, J. Phys. Soc. Jpn. **81**, 064707 (2012).
[18] K. Hubkowska, M. Łukaszewski, and A. Czerwiński, Electrochem. Commun. **20**, 175 (2012).
[19] D. Papaconstantopoulos, B. Klein, E. Economou, and L. Boyer, Phys. Rev. B **17**, 141 (1978).
[20] P. Vargas and N. E. Christensen, Phys. Rev. B **35**, 1993 (1987).
[21] C. Elsässer, J. Zhu, S. G. Louie, M. Fähnle, and C. T. Chan, J. Phys.: Condens. Matter **10**, 5081 (1998).
[22] B. Qi, I. Perez, P. H. Ansari, F. Lu, and M. Croft, Phys. Rev. B **36**, 2972 (1987).
[23] S. Luo, D. Wang, and T. B. Flanagan, J. Phys. Chem. B **114**, 6117 (2010).
[24] H. Noh, T. B. Flanagan, T. Sonoda, and Y. Sakamoto, J. Alloys Compd. **228**, 164 (1995).
[25] H. Noh, W. Luo, and T. B. Flanagan, J. Alloys Compd. **196**, 7 (1993).
[26] J. K. Nørskov, Phys. Rev. B **26**, 2875 (1982).
[27] S. Fujitani, I. Yonezu, T. Saito, N. Furukawa, E. Akiba, H. Hayakawa, and S. Ono, J. Less Common Metals **172**, 220 (1991).